# Broadband femtosecond frequency doubling in random media

R. Fischer, S. M. Saltiel,[a] D. N. Neshev, W. Krolikowski,[b] and Yu. S. Kivshar
*Nonlinear Physics Centre and Laser Physics Centre, Centre for Ultrahigh-bandwidth Devices for Optical Systems (CUDOS), Research School of Physical Sciences and Engineering, Australian National University, Canberra, Australian Capital Territory 0200, Australia*

(Received 29 August 2006; accepted 15 September 2006; published online 7 November 2006)

The authors demonstrate broadband femtosecond phase-matched noncollinear second-harmonic generation (SHG) in strontium barium niobate crystals with random ferroelectric domains. The process is similar to femtosecond SHG in ultrathin crystals, but it results in higher efficiency and exact mapping of the spectrum of the fundamental field into the spectrum of the second harmonics, even for pulses with complex spectral profiles. The observed parametric conversion process can be used as an efficient frequency mapping from infrared to visible for the femtosecond pulse monitoring. © *2006 American Institute of Physics*. [DOI: 10.1063/1.2374678]

Efficient second-harmonic generation (SHG) is known to depend critically on the phase-matching (PM) conditions usually achieved through the crystal birefringence or quasi-phase matching (QPM).[1] However, the PM requirement limits significantly the bandwidth of the SHG processes. It has been shown recently that the use of *disordered nonlinear media* relaxes the stringent matching conditions thus allowing us to achieve an efficient, broad bandwidth regime of the frequency conversion.[2–5] An example of a quadratic nonlinear medium with randomized domain structure is an unpoled strontium barium niobate (SBN) crystal. It grows naturally with random-size ferroelectric domains that allow us to phase match any second-order parametric process including SHG[6] and sum-frequency mixing[7] over a broad spectrum of wavelengths. Without any crystal poling, the limitations of the bandwidth are mainly given by the transparency window of the crystal in the range of 0.4–6 $\mu$m.

The needlelike antiparallel SBN domains are orientated along the $z$ axis of the crystal, and forms a two-dimensional nonlinear photonic structure with a constant linear refractive index but a randomly modulated nonlinear quadratic response.[8–12] The size of the domains varies between 2 and 8 $\mu$m,[13] providing an infinite set of grating vectors $\mathbf{g}$ ( in the $x$-$y$ plane) for the SHG phase matching: $\mathbf{k}_2=2\mathbf{k}_1+\mathbf{g}$, where $\mathbf{k}_1$ and $\mathbf{k}_2$ denote the wave vectors of the fundamental and second-harmonic waves, respectively. These PM conditions result in SHG emitted in a cone[6] or plane[8,9] depending on the mutual orientation of the laser beam and the crystal $z$ axis (see Fig. 1). However, the broadband harmonic generation comes at the price of reduced conversion efficiency. Up to now all measurements have been performed in the long (nanosecond) pulse regimes resulting in a low conversion efficiency and, consequently, limited applicability. The practical application of such a process, however, becomes feasible when short (femtosecond) pulses are employed, resulting in increased efficiency over the pulse bandwidth.

In this letter we report for the first time, to our knowledge, the observation of femtosecond SHG in SBN crystal with random ferroelectric domains. We study both planar and conical emission geometries and analyze the efficiency of the SHG process and its spectral properties, demonstrating that SH exactly maps even complex spectral shape of the fundamental pulse. These results open novel possibilities for spectral monitoring of femtosecond optical signals over the broad spectral range in the near- and far-infrared regions with a single conversion crystal and no temperature or angle tuning.

In our experiments, we use a femtosecond Ti:sapphire oscillator (Mira, Coherent) with pulse width of ~150 fs [full width at half maximum (FWHM)] pulse energies of ~6–7 nJ, repetition rate of 76 MHz, and tunability in the range of 700–900 nm. The beam from the laser (with an average power of 550 mW) is focused inside the $5\times5\times10$ mm$^3$ SBN:60 crystal by a 50 mm focal length lens, resulting in a focal spot of ~74 $\mu$m (FWHM). All sides of the crystal have been polished allowing the observation of the SH radiation from different directions. The spectral properties of the laser and generated SH are measured by a spectrometer (Ocean Optics HR2000) with 0.3 nm resolution.

When the crystal $z$ axis is oriented perpendicular to the propagation direction, the SH radiation is emitted in the $x$-$y$ plane [see Fig. 1(a)]. This is due to the specific PM

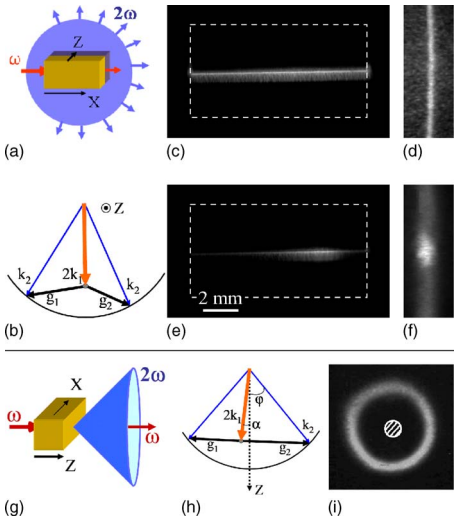


FIG. 1. (Color online) Second-harmonic generation in SBN: [(a)–(f)] SH emission plane for the $z$ axis perpendicular to the beam. [(c) and (d)] SH signal for input power of 250 mW, as seen from (c) top and (d) front. [(e) and (f)] SH at higher input power (425 mW) when the self-focusing process for the fundamental beam leads to local enhancement of SHG. [(g)–(i)] SH conical emission for the $z$ axis parallel to the beam propagation direction. (i) Intensity distribution of the SH beam at 300 mW of input power.

[a]Permanent address: Department of Quantum Electronics, Faculty of Physics, Sofia University, 1164 Sofia, Bulgaria.
[b]Electronic mail: wzk111@rsphysse.anu.edu.au

 

conditions shown in Fig. 1(b), where $\mathbf{g}_1$ and $\mathbf{g}_2$ represent two reciprocal wave vectors. These vectors can be oriented in any direction in the plane perpendicular to the $z$ axis, and their magnitudes are determined by the domain size distribution. In fact, since the latter is of the order of micrometers and the coherence length for the SHG varies between 0.1 and 1.5 $\mu$m, the harmonic generation is clearly due to a high-order QPM. Under such conditions, SH can be emitted in any direction in the plane of Fig. 1(a). As the domain structure of SBN does not contain large-magnitude grating components necessary for the backward SHG process, the signal is emitted predominantly in the forward and transverse directions.

The photographs of the radiation emitted in the transverse and forward directions are shown in Figs. 1(c) and 1(d) for laser power of 250 mW. For the fundamental beam polarized parallel to the $z$ axis, the parametric process is governed by the largest component of the $\chi^{(2)}$ tensor, $d_{33}=12$ pmV. As a result, the SH is also polarized along the $z$ axis. We find that for high input powers (more than 250 mW) the process is strongly affected by the self-focusing of the fundamental beam. The slow time scale of this process points towards its thermal origin.[14,15] Our observation indicates that the formation of an effective nonlinear lens is mediated at the initial stages by local heating of the crystal due to the two-photon absorption of the fundamental beam, and it is followed later by self-phase modulation of the fundamental beam due to the Kerr effect. A signature of the nonlinear lens is visible in Figs. 1(e) and 1(f) as a localized bright spot in the SH signal indicating the position of the focal region of the fundamental beam.

When the fundamental wave propagates along or forms a small angle with the $z$ axis, the SH is emitted in the form of a cone [see Fig. 1(g)]. This is because all reciprocal wave vectors lie in a plane, perpendicular to the propagation $z$ axis. Because of randomness these vectors are uniformly distributed in that plane contributing equally towards the conical emission of the SH. The diagram of the PM conditions for this case is shown in Fig. 1(h), where $\mathbf{g}_1$ and $\mathbf{g}_2$ are again the two possible reciprocal grating wave vectors. However, only a limited number of grating vectors with the magnitudes between $|\mathbf{g}_1|$ and $|\mathbf{g}_2|$ participate in the ring-SHG process. This is in contrast to the previous case of the plane emission, where all grating components contribute to the frequency conversion. Again, because of limited minimal size of domains the QPM is of high- order type, and subsequently the efficiency is low. The longitudinal and transverse PM conditions in this case can be written as $k_2\cos(\varphi)=2k_1\cos(\alpha)$ and $k_2\sin(\varphi)\mp 2k_1\sin(\alpha)=|g_{1,2}|$, respectively, and $\alpha$ and $\varphi$ are defined in Fig. 1(h). The transverse PM condition is always fulfilled, and from the longitudinal PM condition one can find that the cone angle $\varphi$ is a function of both the fundamental wavelength $\lambda_{FF}$ and misalignment angle $\alpha$ of the fundamental beam with respect to the crystal $z$ axis. We note that the SH wave emitted outside the crystal is a cone with an axis always coinciding with the $z$ axis, independently of $\alpha$ and $\lambda_{FF}$. Due to the symmetry of the SHG geometry, the conical emission is always radially polarized.[16,17]

As the next step, we characterize the femtosecond conversion efficiency for both geometries, i.e., a ratio of the generated average output SH power and the input power of the fundamental. Figure 2(a) shows the SHG efficiency in the planar geometry as a function of the power of the fundamental wave, for two different wavelengths of 820 and 860 nm. Because of the difficulties in collecting all power of the generated SH signal, only energy emitted in one of the directions perpendicular to the propagation direction is measured through a short-pass filter. It is evident that for low input power the SHG efficiency increases linearly with the power of the fundamental. This is well expected from the quadratic SH process. However, for the powers higher than 250 mW, the dependence becomes quadratic. This is a direct consequence of the increased intensity of the fundamental due to the thermal self-focusing. In order to quantify the process of fundamental self-focusing, in the same figure we plot the divergence of the fundamental beam measured outside the crystal as a function of the input power. The beam divergence is inversely proportional to the size of the focal spot inside the crystal. Thus, an increased divergence is a direct indication of thermal self-focusing of the beam inside the crystal. Clearly, there is no change of the beam size for the powers below 250 mW. However, when the power exceeds this critical value, the beam divergence increases rapidly. We notice that a change of the slopes for the beam divergence and the conversion efficiency coincide, confirming the scenario of the SHG enhancement.

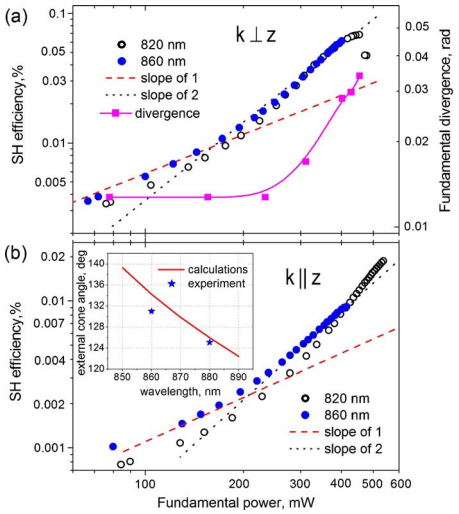


FIG. 2. (Color online) Measured efficiency of the SHG process (in percent) for (a) plane and (b) cone geometries, as a function of the input power, for the wavelengths of 820 and 860 nm. Dashed lines are the expected linear dependencies (slope of one), and dotted lines correspond to a quadratic dependence (slope of two). Squares indicate the measured divergence of the fundamental beam outside the crystal.

As follows from Fig. 2(a), the maximum efficiency of SHG is close to 0.1%. We note that the radiation coming out from the top surface and recorded by the power meter is only a fraction of the whole signal emitted in this plane. Due to the total internal reflection almost half of the power of the generated SH is trapped inside the sample and only emission at the angles in the range of $90\pm 23$ is collected by the power meter. After accounting for the whole generated SH signal we estimate the total conversion efficiency for the planar emission to be 0.38%, which is the highest reported so far. This relatively high, for such a high-order interaction process, efficiency can be explained by high beam intensities (of the order of 10 GWcm$^2$) in the self-focusing region. In addition, because of the noncolinearity of interaction, the output SH signal is an "incoherent" superposition of contributions generated throughout the sample. This leads to linear depen-

dence of SH power on propagation distance of the fundamental wave.

The effective nonlinearities for planar and conical emissions are $d^p_{\text{eff}} \sim d_{33}$ and $d^c_{\text{eff}} \sim d_{31} \sin\varphi$, respectively. In our experiment we have $d^c_{\text{eff}} \approx 0.19 d^p_{\text{eff}}$. Hence, the SHG efficiency of the cone is expected to be significantly lower [it is indeed the case, as seen in Fig. 2(b)]. The measured efficiency ratio (plane/cone) is around 20, close to the theoretically estimated value of 28. The efficiency as a function of the input power of the fundamental wave again reflects an abrupt change of the dependence from linear to quadratic at the critical value of 250 mW of the input power due to thermal self-focusing of the fundamental wave.

The inset in Fig. 2(b) illustrates the important dependence of the angular dispersion of the generated SH cone on the wavelength $\lambda_{FF}$. For $\lambda_{FF}$=860 and 880 nm, the external total conical angles measured at low laser powers are 131° and 125.1°, respectively. This agrees well with theoretically predicted values of 134.24° and 125.95°. A small discrepancy is due to uncertainty in the Sellmeier formula.[18] For high laser powers the cone angle is reduced due to the induction of a thermal lens. Because of the dependence of the conical angle on the wavelength, the propagation of the fundamental beam with a very broad spectral content will result in a conical emission of SH with each spectral component propagating at a specific angle $\varphi(\lambda)$. Due to high wavelength sensitivity, this property can be well considered as *a nonlinear superprism effect*.[19] It should be also mentioned that the angle of the conical emission $\varphi$ increases monotonically with the angle $\alpha$ between the propagation direction of the fundamental wave and the $z$ axis. In the most extreme case when $\alpha \rightarrow \pi 2$, the cone is transformed into a plane.

Since the spectral response of the medium with randomly distributed domains is flat, one may expect that the SHG process will not introduce any spectral distortions in the case of the spectrally broad fundamental wave, even in the case of complex spectral profiles. To verify this hypothesis, we investigate the spectral response of the SH signal for incident beam powers below and above the self-focusing. In the first instance, the spectrum of the fundamental wave is smooth and it is determined by the output characteristics of our laser. On the other hand, for high input powers the spectrum experiences significant broadening and distortions caused by the nonlinear phase modulation due to a direct[20] and cascading[21] third-order nonlinearities. In Fig. 3, we show the spectral profiles of the fundamental and the generated SH pulse for two specific cases of the input powers of 83 and 566 mW. The SH signal is collected either from the top (a) or front [(b) and (c)] facets of the crystal, respectively [see Fig. 1(a) for the measurement geometry]. It is clear that spectra of the second harmonic represent almost exact copies of the fundamental wave. This unique property can be used as an efficient frequency mapping from infrared to the visible for femtosecond pulse monitoring. It represents an ideal tool for noninvasive and alignment-free method for transformation of optical signals from far infrared into the sensitivity window of standard silicon detectors.

In conclusion, we have demonstrated an efficient SHG in an unpoled SBN crystal with random ferroelectric domains. The crystal is phase matched in broad spectral range and no poling is required. Due to a flat spectral response of the crystal, the spectrum of the SH wave exactly maps the spectral profile of the fundamental beam. Such a spectrally nonselective SHG is similar to the SH conversion in an ultrathin crystal, but with highly increased efficiency.

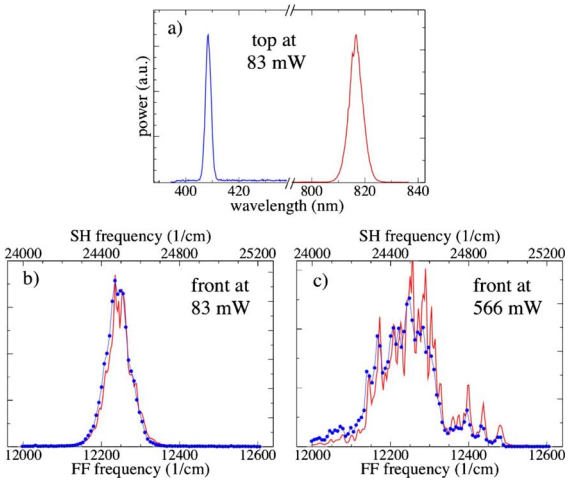


FIG. 3. (Color online) Measured SH (blue with dots) and fundamental at 815 nm (red solid) spectral shapes for different fundamental powers collected either from the (a) top or [(b) and (c)] front facets of the crystal. [(a) and (b)] 83 mW; (c) 566 mW.

The authors acknowledge support of the Australian Research Council.

[1] M. M. Fejer, G. A. Magel, D. H. Jundt, and R. L. Byer, IEEE J. Quantum Electron. **QE-28**, 2631 (1992).
[2] M. Baudrier-Raybaut, R. Haïdar, Ph. Kupecek, Ph. Lemasson, and E. Rosencher, Nature (London) **432**, 374 (2004).
[3] S. E. Skipetrov, Nature (London) **432**, 285 (2004).
[4] E. Yu. Morozov, A. A. Kaminskii, A. S. Chirkin, and D. B. Yusupov, JETP Lett. **73**, 647 (2001).
[5] X. Vidal and J. Martorell, Phys. Rev. Lett. **97**, 013902 (2006).
[6] A. R. Tunyagi, M. Ulex, and K. Betzler, Phys. Rev. Lett. **90**, 243901 (2003).
[7] J. J. Romero, D. Jaque, J. García Solé, and A. A. Kaminskii, Appl. Phys. Lett. **81**, 4106 (2002).
[8] M. Horowitz, A. Bekker, and B. Fischer, Appl. Phys. Lett. **62**, 2619 (1993).
[9] S. Kawai, T. Ogawa, H. S. Lee, R. C. DeMattei, and R. S. Feigelson, Appl. Phys. Lett. **73**, 768 (1998).
[10] V. Berger, Phys. Rev. Lett. **81**, 4136 (1998).
[11] N. G. R. Broderick, G. W. Ross, H. L. Offerhaus, D. J. Richardson, and D. C. Hanna, Phys. Rev. Lett. **84**, 4345 (2000).
[12] S. M. Saltiel, A. A. Sukhorukov, and Yu. S. Kivshar, Prog. Opt. **47**, 1 (2005).
[13] J. J. Romero, C. Aragó, J. A. Gonzalo, D. Jaque, and J. García Solé, J. Appl. Phys. **93**, 3111 (2003).
[14] M. Horowitz, R. Daisy, O. Werner, and B. Fischer, Opt. Lett. **17**, 475 (1992).
[15] D. Kip, E. Kratzig, V. Shandarov, and P. Moretti, Opt. Lett. **23**, 343 (1998).
[16] R. Dorn, S. Quabis, and G. Leuchs, Phys. Rev. Lett. **91**, 233901 (2003).
[17] A. R. Tunyagi, Ph.D. thesis, University of Osnabrück, 2004.
[18] Th. Woike, T. Granzow, U. Dörfler, Ch. Poetsch, M. Wöhlecke, and R. Paukrath, Phys. Status Solidi A **186**, R13 (2001).
[19] H. Kosaka, T. Kawashima, A. Tomita, M. Notomi, T. Tamamura, T. Sato, and S. Kawakami, Phys. Rev. B **58**, R10096 (1998).
[20] M. Sheik-Bahae, D. C. Hutchings, D. J. Hagan, and E. W. Van Stryland, IEEE J. Quantum Electron. **27**, 1296 (1991).
[21] X. Liu, F. O. Ilday, K. Beckwitt, and F. W. Wise, Opt. Lett. **25**, 1394 (2000).